Int J CARS (2006) 1:205–212
DOI 10.1007/s11548-006-0058-0

ORIGINAL ARTICLE

An improved needle steering model with online parameter estimator

Kai Guo Yan · Tarun Podder · Di Xiao · Yan Yu · Tien-I Liu · CWS Cheng · Wan Sing Ng

Received: 8 August 2006 / Accepted: 29 September 2006 / Published online: 16 November 2006

Abstract
Purpose Needle steering can improve targeting accuracy and guide the tip to areas that are currently not accessible. This paper proposes and validates a steering model to be capable of predicting the system dynamics during needle-tissue contact procedure.
Methods The spring-beam-damper needle steering model we proposed has been extended with depth-varying mean parameters considering the tissue inhomogeneity. Local polynomial approximations in finite depth segments were adopted to estimate the unknown depth-varying mean parameters. Based on this approach, an online parameter estimator has been designed using modified least square method with forgetting factor to estimate the parameters using the online measured dataset.
Results Extensive experiments have been carried out in various phantoms to validate the improved needle steering model based on online experiment data. Results have shown that the model can track the needle tip trajectory with satisfactory accuracy even in the presence of large disturbances and noises. The convergence rate and estimation accuracy can be greatly improved when a needle is suitably supported.
Conclusion The model can give satisfactory prediction if the input data are properly collected to avoid the sensor noises.

Keywords Needle guidance · Percutaneous intervention · Spring-beam-damper needle steering model

K. G. Yan (✉) · W. S. Ng
Schools of Mechanical & Aerospace Engineering,
Nanyang Technological University, Singapore, Singapore
e-mail: yank0001@ntu.edu.sg

T. Podder · Y. Yu
Department of Radiation Oncology,
Thomas Jefferson University Hospital, Philadelphia, PA, USA

D. Xiao
Department of Surgery,
National University Hospital, Singapore,
Singapore

T.-I. Liu
Computer Integrated Manufacturing Lab,
California State University, Sacramento, CA, USA

C. W. S. Cheng
Department of Urology, Singapore General Hospital,
Singapore, Singapore

Introduction

Precise needle insertion is very important for a number of percutaneous interventions. Yet it is very difficult to achieve in practice. Errors caused by the target movement and needle deflection have been observed for a long time [1,2]. Yet to date, there are few effective physical-based needle steering systems existing for correcting the needle deflection when it occurs. In addition, many procedures are currently not amenable to needles because of obstacles such as bone or sensitive tissues, which lie between feasible entry points and potential targets. Thus, there is a clear motivation for needle steering in order to provide accurate and dexterous targeting.

Flexible needle steering was first addressed by DiMaio [3]. He used a large-strain elastic needle model coupled with the two-dimensional tissue models to simulate the needle and tissue phantom reaction during

needle insertion, as well as to predict target motion and needle trajectories due to phantom deformation and needle deflection. The traditional finite element model was used to solve the system kinematics. The model was later extended by other researchers to three-dimensional models [4,5].

In 2005 Medical Image Computing and Computer-Assisted Intervention (MICCAI) conference, Daniel Glozman and Moshe Shoham [6] presented a simplified virtual spring model for the needle insertion procedure. They assumed small tissue displacement and linear lateral force response. Modeling of a flexible needle was based on the assumption of quasi-static motion and a third-order polynomial was used to calculate the displacement of each element. Compromise had to be made between the computation efficiency and the model accuracy.

Needle steering making use of the needle bending has also been explored in the past few years. Some researchers have generated needle bending using different strategies such as incorporating a pre-bent stylet inside a straight canula [7], or a telescoping double canula where the internal canula is pre-bent [8]. Other researchers showed that needles with bevel tips bend more than symmetric-tip needles [9]. Making use of this effect, highly flexible bevel-tip slender needles using Nitinol was developed and a nonholonomic model was built accordingly for steering flexible bevel-tip needles in rigid tissues [10]. The nonholonomic model, a generalization of a 3 degree-of-freedom (DOF) bicycle model, was experimentally validated using a very stiff tissue phantom. Recent advances in this nonholonomic model include stochastic model-based motion planning to compensate for noise bias [11], probabilistic models of dead-reckoning error in nonholonomic robots [12], a diffusion-based motion planning to search for a feasible path in full 3D space [13], and motion planning under Markov Motion Uncertainty using dynamic programming to search for a feasible route while avoiding obstacle [14].

In the first BioRob conference held in 2006 in Italy, we proposed a spring-beam-damper needle steering model, in which the tissue reaction was represented by continuously distributed spring-damper system and the flexible needle was assumed to follow the Bernoulli–Euler beam model [15]. The proposed spring-beam-damper model took into consideration both the linear and viscous tissue reaction effects when interacting with the flexible needle. But the spring and damper coefficients were assumed to be constant for simplicity. Considering the tissue inhomogeneity, in this paper, we improve the needle steering model with depth-varying mean parameters to calculate the spring and damper effects. Based on this approach, local polynomial approximations in finite depth segments are used to approximate the unknown depth-varying mean parameters. To estimate the parameters in the model, an online parameter estimator has been designed using modified least square method with forgetting factor. Extensive experiments have been carried out in various phantoms to validate the improved needle steering model with the online parameter estimator. Results have shown that the improved needle steering model with the online parameter estimator can track the needle tip trajectory with fast convergent rate and satisfactory accuracy if the input data are properly collected to avoid the sensor noises. The details are reported in the following sections. Conclusions and future works are given at the end.

Improved needle steering model with depth-varying coefficients

The dynamic equations of needle steering model

A spring-beam-damper system as shown in Fig. 1 is considered in this study to model the system dynamics between the lateral steering forces acting at the needle base and the corresponding needle tip lateral movement during insertion into the soft tissue. The flexible needle is assumed to follow the Bernoulli–Euler beam model and to be clamped tightly at the base. The rectangle in Fig. 1 is used to represent the human tissue. The tissue reaction force is represented using the virtual continuously distributed spring-damper system. The initial lengths of springs are decided by the needle tip trajectory as shown in Fig. 1. At the beginning, the needle is placed next to the tissue. With time progressing on, the needle inserts into the tissue. When lateral force is applied at the needle base, the needle will move laterally. Thus the spring-damper system will come into contact

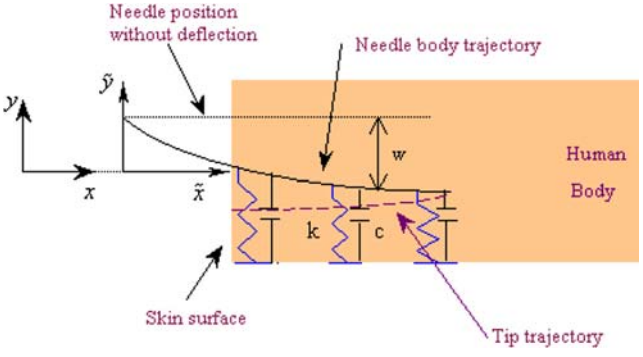

Fig. 1 Mechanism of the spring-beam-damper system for the needle insertion procedure

with the needles and exert forces on it. The forces of the springs at time instant t are determined by the needle body shape at that time and the needle tip trajectory while the forces of the dampers are determined by the velocities of the contact points. During this procedure, not only the tissue deformation and the needle flexibility, but also their interaction effects should be taken into consideration.

The system dynamic equation can be derived using Hamilton's principle as follows:

$$\int_{t_1}^{t_2} (\delta T - \delta V + \delta W_{\mathrm{nc}})\mathrm{d}t = 0 \tag{1}$$

where T is kinetic energy, V is potential energy and W_{nc} is work done by nonconservative forces.

To facilitate the modeling procedure, a local coordinate system was introduced by the Galilean transformation to replace the fixed coordinates (x) with a moving coordinate system ($\tilde{x}$), which is attached at the needle base and moves with it, as shown in Fig. 1. Unconstrained modal analysis was adopted to solve the dynamic equations. After some algebraic manipulations (refer to [15] for more details), the model can finally be derived as below.

$$M\ddot{x} + c\Pi\dot{x} + (k\Pi + \Pi_1)x = u - kH \tag{2}$$

where

$$x = \begin{pmatrix} \alpha \\ q \end{pmatrix}, \quad M = \begin{pmatrix} M_t & 0 \\ 0 & 1 \end{pmatrix}, \quad u = \begin{pmatrix} 1 \\ \beta \end{pmatrix} F_y,$$

$$\Pi_1 = \begin{pmatrix} 0 & 0 \\ 0 & \xi^2 \end{pmatrix}$$

$$\Pi = \begin{pmatrix} v_x t & \int_{L-v_x t}^{L} \varphi(\tilde{x})\mathrm{d}\tilde{x} \\ \int_{L-v_x t}^{L} \varphi(\tilde{x})\mathrm{d}\tilde{x} & \int_{L-v_x t}^{L} \varphi^2(\tilde{x})\mathrm{d}\tilde{x} \end{pmatrix},$$

$$H = \begin{pmatrix} \int_0^t y_1(t_1)v_x\mathrm{d}t_1 \\ \int_0^t \varphi_1(v_x t_1 + L - v_x t)y_1(t_1)v_x\mathrm{d}t_1 \end{pmatrix}$$

where α describes the motion of the center of mass of the total system without perturbation, q is the time-varying amplitude of motion, M_t is the total mass of the fixture and needle, ξ is the natural frequency of the system, L is the length of the elastic beam, $v_x$is needle insertion velocity, which is assumed to be constant for modeling simplicity. F_y is the lateral steering force, which acted at the needle base in y direction. k is stiffness coefficient of the spring per unit length, and c is the damper coefficient per unit length. y_1 refers to the needle tip trajectory, β is defined to satisfy

$$\beta = -\frac{\rho}{M_t}\int_0^L \phi(\tilde{x})\mathrm{d}\tilde{x} \tag{3}$$

and

$$\varphi(\tilde{x}) = \beta + \phi(\tilde{x}) \tag{4}$$

where $\phi(\tilde{x})$ is the shape function.

Local polynomial approximation of the depth-varying mean parameters

Considering the inhomogeneous human tissue and the multiple tissue layers that the needle will penetrate through during surgery, here we propose to use depth-varying mean parameters to calculate the spring/damper reaction forces and use local polynomials to approximate the depth-varying mean parameters.

Assumption 1:
The spring and damper coefficients are different at different depth of the tissue. At each insertion step, the spring/damper effects along the needle body that is inside the tissue can be calculated using mean spring/damper coefficients $\theta(s) = [\,\bar{c}\ \bar{k}\,]^{\mathrm{T}}$. These mean coefficients will vary with each step.

This assumption takes into considerations the inhomogeneous human tissue, and at the same time, reduces the computation intensity using mean values to calculate the spring/damper force along the needle body at each insertion step. Furthermore, the adoption of the mean values guarantees that $\theta(s)$ is continuously distributed regardless of the abrupt change of the tissue properties, e.g. pathological changes of the tissue, or multi-layer insertion.

Assumption 2:
The depth-varying mean parameters $\theta(s)$ can be represented by a serials of local polynomial approximations in finite segments.

This can be justified using Taylor series expansion. Recall that the functions $\theta(s)$ can be expanded around certain points s_0 as shown below.

$$\theta(s) = \theta(s_0) + (s - s_0)\theta^{(1)}(s_0) + \cdots + \frac{(s - s_0)^p}{p!}\theta^{(p)}(s_0) + \int_{s_0}^{s} \frac{(s - \xi)^{p+1}}{(p+1)!}\theta^{(p+1)}(\xi)\mathrm{d}\xi \tag{5}$$

Here, $\theta(s)$ is approximated by the first $p + 1$ terms. The last term represents the error due to the approximation.

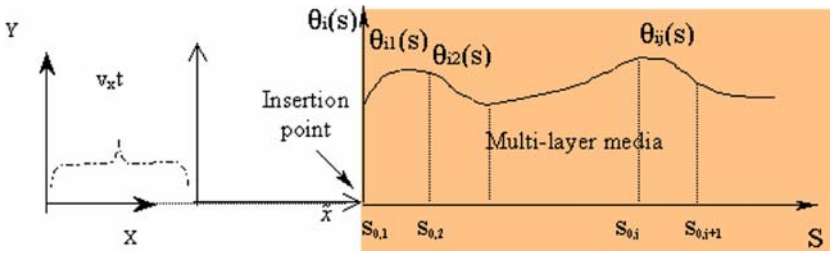

Fig. 2 Local polynomial approximations of the parameter functions

From the above assumptions, we can divide the whole insertion length into several segments and adopt piecewise continuous p-order differentiable functions θ_{ij}, $i = 1,2$, $j = 1,2,\ldots,n$ to represent the depth-varying mean parameter $\theta_i(s), i = 1,2$ in each segment, as illustrated in Fig. 2. Here, the index i refers to the ith parameter (spring or damper coefficient); while the index j refers to the jth segment and n is the number of segments. S coordinate system is adopted for convenient representation of the parameters. The origin of the S coordinate system is set at the insertion point, as shown in Fig. 2. The transformation between S domain and $\tilde{x}$ domain is given by

$$\begin{cases} \tilde{x} = s + L - \dot{s}t \\ \dot{s} = v_x \end{cases} \tag{6}$$

under the assumption that the needle is inserted at constant velocity.

Thus the polynomial approximation of θ_{ij} is represented as

$$\begin{aligned} \theta_{ij}(s) &= a_{ij0}(s_{0,j}) + a_{ij1}(s_{0,j})(s - s_{0,j}) \\ &\quad + \cdots + a_{ijp}(s_{0,j})(s - s_{0,j})^p \\ &:= \sum_{k=0}^{p} a_{ijk}(s_{0,j})(s - s_{0,j})^k, \quad s \in [s_{0,j}, s_{0,j} + l) \\ &:= \varphi_{ij}^{\mathrm{T}}(s, s_{0,j}) A_{ij}(s_{0,j}), \end{aligned} \tag{7}$$

where $l$is the length of the segment and p is the order of the polynomial. $s_{0,j}$ refers to the resetting depth at which the jth window of the local polynomial approximation for parameter θ_i begins. $s_{0,j}$is given by the sequence $s_0 = \{s_{0,j}\}, j = 1,\ldots,n$ and $s_{0,(j+1)} - s_{0,j} = l$. $a_{ijk}(s_{0,j}) = (1/k!)\theta_{ij}^{(k)}(s_{0,j}), k = 0,\ldots,p$, $\theta_{ij}^{(k)}(s_{0,j})$is the kth depth derivative evaluated at $s = s_{0,j}$. $A_{ij}(s_{0,j}) := [a_{ij0}(s_{0,j}), a_{ij1}(s_{0,j}), \ldots, a_{ijp}(s_{0,j})]^{\mathrm{T}}$ is the unknown constant vector and $\varphi_{ij}^{\mathrm{T}}(s, s_{0,j}) := [1, (s - s_{0,j}), \ldots, (s - s_{0,j})^p]$ is a column vector. Notice that $A_{ij}(s_{0,j})$ is constant only within each segment $[s_{0,j}, s_{0,j+1})$ and in general differs from one segment to another for the inhomogeneous tissue.

Therefore, it is possible to use Eq. (7) to approximate $\theta_{ij}(s)$ more precisely by choosing either a higher order polynomial, that is, p large, or a smaller segment l, or both. If we partition the whole insertion length into segments with the length of each segment equal to l, then the depth-varying function $\theta_i(s)$ can be approximated by a number of polynomials $\theta_{ij}(s)$ located in each segment with constant coefficients a_{ijk}, as shown in Eq. (7).

Online parameter estimator design

Discretization of the needle steering force model

The discretized needle steering model is considered here. The needle steering model can be reorganized as

$$Y_k = \Phi_{k-1}^{\mathrm{T}} \bar{\theta} \tag{8}$$

where $\Phi_{k-1}^{\mathrm{T}} = [-TBM^{-1}\Pi_{k-2}B^{-1}(Y_{k-1} - Y_{k-2}) - T^2BM^{-1} \times (\Pi_{k-2}B^{-1}Y_{k-2} + H_{k-2}) \quad 2Y_{k-1} - Y_{k-2} + T^2BM^{-1}u_{k-2} - BM^{-1}\Pi_{1k}B^1Y_{k-2}]$, $\bar{\theta} = [\bar{c}\ \bar{k}\ 1]^T \in R^m$ is the unknown depth-varying mean parameter vector with an additional constant 1. The constant comes from reorganization of the system model as the shown pattern. Substituting Eq. (7) into Eq. (8), and discretizing the model with $t = kT$(T, sampling time), we can get

$$\begin{aligned} Y_k &= \Phi_{k-1}^{\mathrm{T}}\theta = \underbrace{\Phi_{k-1}^{\mathrm{T}} \begin{bmatrix} \varphi^{\mathrm{T}}(k, k_{0,j}) & & \\ & \varphi^{\mathrm{T}}(k, k_{0,j}) & \\ & & 1 \end{bmatrix}}_{X_{k-1}^{\mathrm{T}}} \underbrace{\begin{bmatrix} A_1 \\ A_2 \\ 1 \end{bmatrix}}_{\vartheta} \\ &:= X_{k-1}^{\mathrm{T}}\vartheta \end{aligned} \tag{9}$$

Online parameter estimator using modified least square with forgetting factor

Currently, an effective equipment or technique that can test the virtual spring and damper coefficients of the human tissue is not available, especially for real time operation. Thus we design an online parameter estimator to facilitate the estimation of the parameters. The parameter estimator is designed in such a way that it can determine the parameter vector $\hat{\vartheta}$ that will induce minimum errors from the computed and measured steering

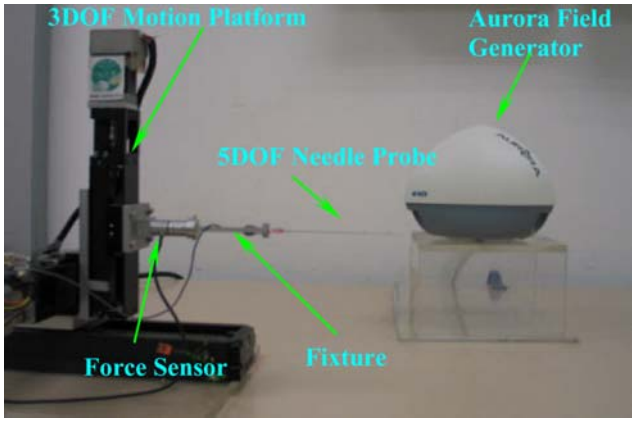

Fig. 3 Experimental setup

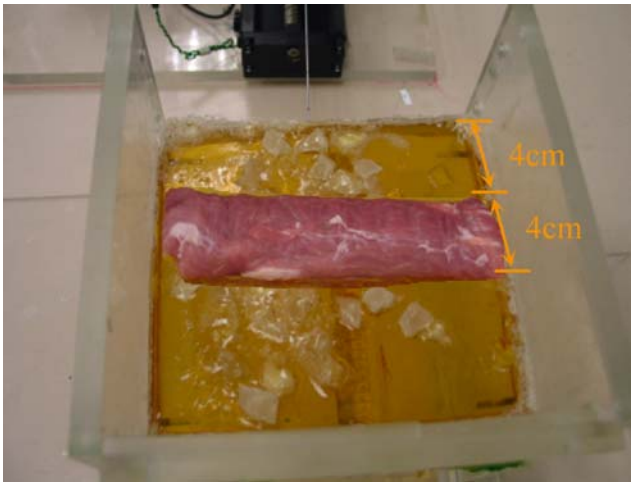

Fig. 4 Two-layer phantom. First layer: inhomogeneous phantom with thickness 4cm. Second layer: animal meat with thickness 4cm

model output in the sense of least square, where $\hat{\vartheta}$ is the estimate of ϑ. The modified least-square estimation with covariance resetting and forgetting factor is adopted to design this online parameter estimator, which takes the form:

$$\begin{aligned} \vartheta_k &= \vartheta_{k-1} + K_k(Y_k - \mathrm{X}_{k-1}^{\mathrm{T}}\,\hat{\vartheta}_{k-1}) \\ K_k &= P_{k-1}X_{k-1}[\lambda I + \mathrm{X}_{k-1}^{\mathrm{T}}P_{k-1}X_{k-1}]^{-1} \\ P_k &= [P_{k-1} - K_k\mathrm{X}_{k-1}^{\mathrm{T}}P_{k-1}]/\lambda \end{aligned} \tag{10}$$

where P_k and K_k are the computed covariance matrix and gain respectively at step k. λ is the forgetting factor.

Experimental validation

Materials and methods

To validate the effectiveness of the proposed steering model, physical experiments were carried out. The experimental setup shown in Fig. 3 was used to carry out the experiment. The 3DOF motion platform can drive the needle to follow some pre-determined trajectories. A 6 DOF force/torque (F/T) sensor (Nano 17-SI-12-0.12® from ATI Industrial Automation, USA) is mounted at the needle base to measure the needle base force. The needle adopted here is a 5-DOF MagTrax Needle Probe (from Traxtal Technology, Canada). It is 130 mm in length, has a trihedral tip and a 19G stylet with 18G cannula. It has one sensor located at the stylet's distal. The movement of the needle tip can be observed in real time via an electromagnetic system called Aurora® (from Northern Digital Inc., Canada); while the needle base position can be calculated from motor runs.

An "active" way of validating the proposed model by steering the needle tip to a defined position is infeasible now, since it will require a steering strategy, which is our future task. Instead, a "passive" way of validation was adopted to show that the model could accurately predict the needle tip trajectory when giving some inputs—needle base lateral forces.

The needle was driven into the prepared phantom by the 3DOF platform following some pre-designed trajectories with various insertion speeds. The needle tip/base positions and corresponding needle base force data were collected during the procedure. These collected datasets were first passed through a designed filter to remove the measurement noises and smooth the data. After that, the datasets went through the designed online parameter estimator to estimate the parameters. At the same time, the model was simulated using the online estimated parameters and the collected dataset to predict the output, the needle tip position. Last, the simulated outputs, the needle tip position data, were compared with the measured position data to check the effectiveness of the steering model.

Experimental results and discussions

Extensive experiments have been carried out in various phantoms including pure gelatin phantoms, animal tissue phantoms, artificial inhomogeneous phantoms and two-layer phantoms. The results have shown similar patterns. For the space constraint, here we present the results in the two-layer phantom.

A two-layer phantom was made to simulate the multilayer insertion during surgery as shown in Fig. 4. The first layer was made of gelatin phantom with different stiffness PVC lumps, unsolved gelatin lumps and bubbles inside to represent the glands, tumors, vessels and nerves, etc., which may exist in the tissue while the

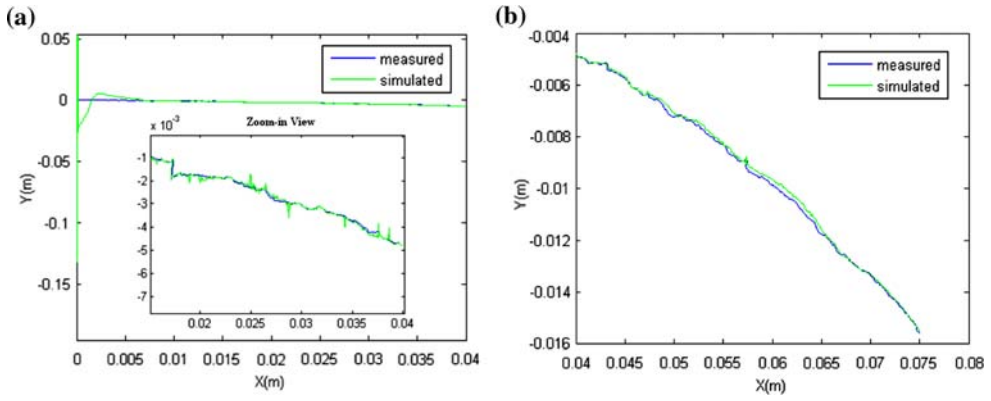

Fig. 5 Simulations in two-layer phantom (without support): **a** Simulation result in the first segment. **b** Simulation result in the second segment

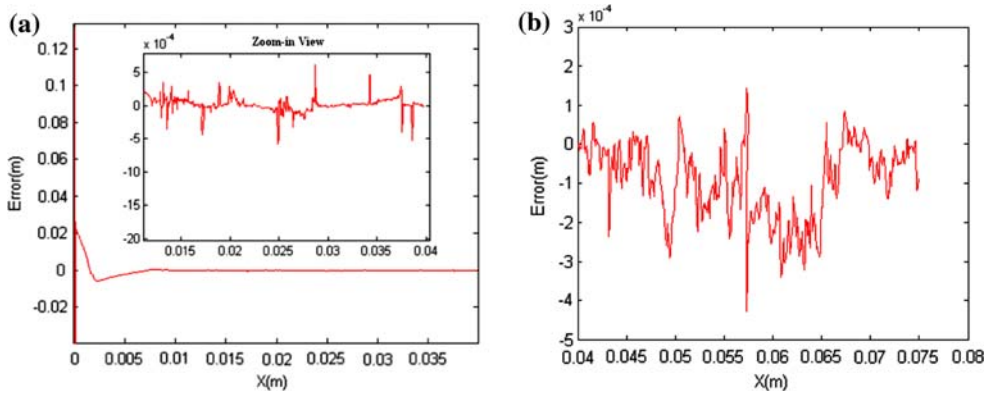

Fig. 6 Simulation errors in two-layer phantom (without support): **a** Simulation errors in the first segment. **b** Simulation errors in the second segment

second layer was made by the animal meat (pork). The thicknesses of the two layers were both around 4 cm.

Needle insertion without support

The needle was first driven into the phantom for 8 cm in x direction, and 2 cm in y direction. The insertion speed was set to be 8, 4 and 2 mm/s, respectively. The lateral speed was chosen accordingly in order to keep the movements in x and y to start and stop simultaneously. During the procedure the needle tip/base position data and corresponding needle base forces were collected for analysis.

Fifth order polynomials were chosen to represent the spring and damper coefficients. The initial coefficients were set to be [3 × 105 × ones (6,1); 2 × 106 × ones (6,1); 1]. The initial covariance matrix was set to be [1016 × eye (13,12) zeros (13,1)]. The forgetting factor was selected to be 0.99. Two segments were chosen corresponding to the two layers. The simulated tip trajectories vs. the measured ones in these two segments and corresponding errors are shown in Figs. 5 and 6.

From the above figures, we can see that the errors at the beginning are quite large, but after convergence, the accuracy is satisfactory. The large estimation errors at the beginning have been investigated, which are mainly due to the poor initial estimation and the noisy sensor output caused by the sudden oscillation of the long slender needle. An accurate initial estimation is hard to achieve especially in applications involving complex biological tissue. But the oscillation of the needle can be depressed by adding support to the needle. Therefore, another experiment was designed and carried out to test the model performance when the needle got supported during steering procedure.

Needle steering with support

In this experiment, the needle was first inserted into the phantom for some distance before the lateral movement. Thus when the lateral movement was actuated,

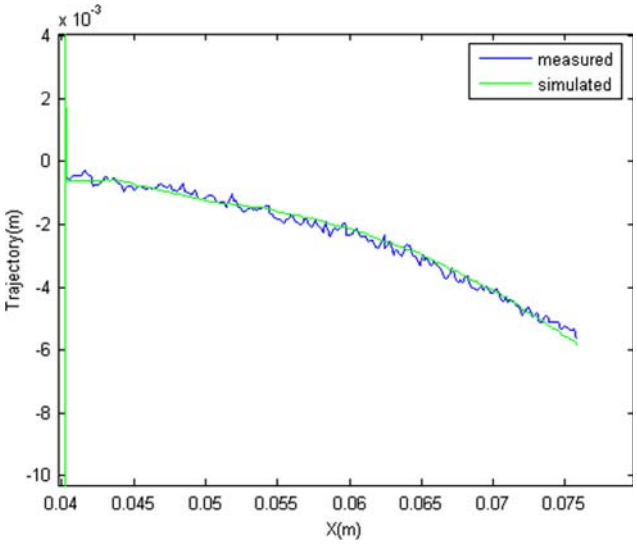

Fig. 7 Simulations in two-layer phantom (with support)

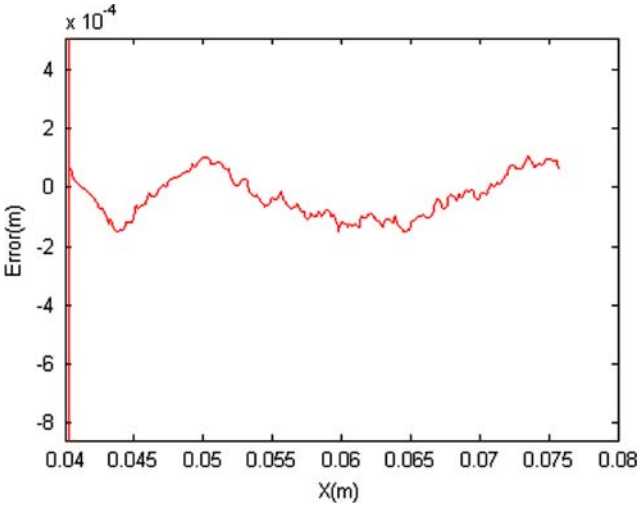

Fig. 8 Simulation errors in two-layer phantom (with support)

part of the needle body had already been inside the phantom, which acted as a support to the needle body. This procedure is more like what is performed in the real surgery: normally a straight-line needle insertion is performed at the start. The needle steering will only be actuated when the needle is found deviating from its planed trajectory, by which time part of the needle has already been inside the tissue. The same initial settings were chosen as in Sect. Needle insertion without support Figures 7 and 8 show the estimation results. Even though at the beginning the error is still large due to the initial estimation, it converges very fast and the accuracy is greatly improved. Thus we can expect the model to give satisfactory prediction if the input data are properly collected to avoid the sensor noises.

Conclusion and future work

In this work, a spring-beam-damper needle steering model with depth-varying mean parameters is considered to model the system dynamics during the needle–tissue contact procedure. Local polynomials in finite segments are adopted to approximate the unknown depth-varying mean parameters. The accuracy of the approximation depends on the order of the polynomial and the width of the segment, which can be chosen. The polynomial coefficients vary from one segment to the other, but within a segment they are constant. Thus, each depth-varying parameter can be approximated independently in each segment by a set of constant coefficients. This local polynomial method is more data-centric and depends on the window of the chosen segment in which the data are being collected.

Based on this approach, an online parameter estimator has been designed using modified least square method with forgetting factor. Extensive experiments have been carried out in various phantoms to validate the improved needle steering model based on online experiment data. Results have shown that the model can track the needle tip trajectory with satisfactory accuracy even in the presence of large disturbances and noises. The estimation errors at the beginning are large due to the poor initial estimation and the noisy sensor output caused by the sudden oscillation of the long slender needle. To solve this problem, experiments with the 'supported' needle were carried out by making use of the tissue as the support. Results have shown that the convergence rate and overall accuracy have been greatly improved. Thus we can expect the model to give satisfactory prediction if the input data are properly collected to avoid the sensor noises.

In future, we will use the proposed steering model with the online parameter estimator to design an adaptive steering system that can direct the needle tip to a prescribed position.

Acknowledgements Nanyang Technological University (Singapore), National Medical Research Council of Singapore 0859/2004 and US National Cancer Institute (NCI) (under grant R01 CA091763) are acknowledged for financial support.

References

1. Pouliot J, Taschereau R, Cot′e C, Roy J, Tremblay D (1999) Dosimetric aspects of permanent radioactive implants for the treatment of prostate cancer. Phys Can 55:61–68
2. Alterovitz R, Pouliot J, Taschereau R, Hsu I-C, Goldberg K (2003) Needle insertion and radioactive seed implantation in human tissues: simulation and sensitivity analysis. In: Pro-

ceedings of IEEE international conference on robotics and automation 2:1793–1799
3. DiMaio SP (2003) Modelling, simulation and planning of needle motion in soft tissues, PhD thesis, The University of British Columbia
4. Hing J, Brooks AD, Desai JP (2005) Reality-based estimation of needle and soft-tissue interaction for accurate haptic feedback in prostate brachytherapy simulation. In: International symposium of robotics research, San Francisco
5. Goksel O (2005) 3D needle-tissue interaction simulation for prostate brachytherapy. In: proceedings of the 15th annual canadian conference on intelligent systems, pp 827–834
6. Glozman D, Shoham M (2004) Flexible needle steering and optimal trajectory planning for percutaneous therapies. In: proceedings of MICCAI pp 137–144
7. Ebrahimi R, Okzawa S, Rohling R, Salcudean S (2003) Hand-held steerable needle device. In: Proceedings of MICCAI, pp 223–230
8. Daum W (2003) A deflectable needle assembly. Patent 5,572,593
9. O'Leary MD, Simone C, Washio T, Yoshinaka K, Okamura AM (2003) Robotic needle insertion: effects of friction and needle geometry. In: Proceedings of IEEE international conference on robotics and automation, pp 1774–1780
10. Webster III RJ, Cowan NJ, Chirikjian G, Okamura AM (2005) Nonholonomic modeling of needle steering. In: proceedings of the 9th international symposium on experimental robotics
11. Zhou Y, Chirikjian GS (2004) Planning for noise-induced trajectory bias in nonholonomic robots with uncertainty. In: Proceedings of IEEE international conference on robotics and automation, pp 4596–4601
12. Zhou Y, Chirikjian GS (2003) Probabilistic models of deadreckoning error in nonholonomic mobile robots. In: Proceedings of IEEE international conference on robotics and automation, pp 1594–1599
13. Park W, Kim JS, Zhou Y, Cowan NJ, Okamura AM, Chirikjian GS (2005) Diffusion-based motion planning for a nonholonomic flexible needle model. IEEE international conference on robotics and automation, pp 4611–4616
14. Alterovitz R, Lim A, Goldberg K, Chirikjian GS, Okamura AM (2005) Steering flexible needles under Markov motion uncertainty. In: Proceedings of IEEE/RSJ international conference on intelligent robots and systems (IROS), pp 120–125
15. Yan K, Sing Ng W, Yu Y, Podder T, Liu T-I, Cheng CWS, Voon Ling K (2006) Needle steering modeling and analysis using unconstrained modal analysis. In: Proceedings of the first IEEE/RAS-EMBS international conference on biomedical robotics and biomechatronics, Italy